Target normal single-spin asymmetry in inclusive electron-nucleon scattering with two-photon exchange: Analysis using $1/N_c$ expansion

J. L. Goity[b,a], C. Weiss[b], C. Willemyns[c]

[a]Department of Physics, Hampton University, Hampton, VA 23668, USA
[b]Theory Center, Jeerson Lab, Newport News, VA 23606, USA
[c]Service de Physique Nucléaire et Subnucléaire, Université de Mons, UMONS Research Institute for Complex Systems, Place du Parc 20, 7000 Mons, Belgium

Abstract

We calculate the target normal single-spin asymmetry caused by two-photon exchange in inclusive electron-nucleon scattering in the resonance region. Our analysis uses the $1/N_c$ expansion of low-energy QCD and combines N and Δ intermediate and final states using the emerging spin-flavor symmetry. The normal spin asymmetry is found to be of the order $\sim 10^{-2}$ and has dierent sign in ep and en scattering. It can be measured in electron scattering at lab energies ∼1–3 GeV and provides a clean probe of two-photon exchange dynamics.

1. Introduction

Electron scattering represents a principal tool for exploring hadron structure and strong interaction dynamics. The process is traditionally described in leading order of the electromagnetic coupling (one-photon exchange approximation), where the amplitude is proportional to the transition matrix element of the electromagnetic current operator between the hadronic states. Recent developments in experiment and theory point to need to include higher-order interactions between the electron and the hadronic system (two-photon exchange) in certain observables [1]. Measurements of the proton form factor ratio G_E^p/G_M^p at Jeerson Lab using the Rosenbluth separation and polarization transfer methods show discrepancies that have been associated with two-photon exchange [2, 3, 4]. A direct demonstration of two-photon exchange becomes possible through compari-son of electron and positron scattering in experiments at DESY [5, 6] and Jeerson Lab [7]. Two-photon exchange is also dis-cussed in connection with muon scattering at MUSE [8]. It also plays an important role in radiative corrections to observ-ables of parity-violating electron scattering [9]. Two-photon exchange has thus become as field of research in its own right.

A particularly interesting observable is the target spin dependence in inclusive electron-nucleon scattering,

$$e(k_1) + N(p_1) \to e(k_2) + X(p_2); \qquad (1)$$

where X denotes the hadronic final states accessible at the incident energy, which are summed over. If the electron is unpolarized, and the nucleon is polarized with a spin 4-vector a_1, with $a_1^2 = -1$ for complete polarization, the dependence of the dierential cross section on the nucleon spin is of the form [10]

$$\frac{d\sigma}{d\Gamma} = \frac{d\sigma_U}{d\Gamma_2} - (e_N a_1)\frac{d\sigma_N}{d\Gamma}\,(2)^{\,2} \qquad (2)$$

($d\Gamma_2$ denotes the invariant phase space element of the final electron and will be specified below). Here e_N is the normalized pseudovector formed from the initial and final electron and the inital nucleon momenta,

$$e_N^{\mu} \equiv \frac{\epsilon^{\mu\nu\rho\sigma} p_{1\nu} k_{2\rho} k_{1\sigma}}{N}; \quad e_N^2 = -1: \qquad (3)$$

In the nucleon rest frame, $p_1 = 0$, the polarization vector is $a_1 = (0; 2S_1)$, with $|S_1| = 1/2$ for complete polarization. The vector e_N is the normal vector to the scattering plane

$$e_N = (0; \mathbf{e}_N); \quad \mathbf{e}_N = \frac{\mathbf{k}_2 \times \mathbf{k}_1}{|\mathbf{k}_2 \times \mathbf{k}_1|}; \qquad (4)$$

and the cross section Eq. (2) depends on the normal component of the nucleon spin, $-(e_N a_1) = 2\mathbf{e}_N \cdot \mathbf{S}_1$. [The same form applies in any frame in which the 3-momenta $\mathbf{k}_1$; $\mathbf{k}_2$ and $\mathbf{p}_1$ lie in a plane, e.g. the electron-nucleon center-of-mass (CM) frame, where $\mathbf{p}_1 + \mathbf{k}_1 = 0$.] The spin-dependent cross section σ_N is zero in one-photon exchange approximation, as a consequence of the hermiticity of the electromagnetic current operator [11], and represents a pure two-photon exchange observable. It is proportional to the imaginary (absorptive) part of the eN → eX two-photon exchange amplitude, which is given by the product of on-shell matrix elements between the initial, intermediate, and final electron-hadron states. Unlike the real (dispersive) part, the imaginary part of the two-photon exchange amplitude is infrared–finite and can be considered separately from real photon emission into the final state [10].

Measurements of the normal spin asymmetry (the ratio of the N and U cross sections) have been performed in deep-inelastic electron scattering on proton [12] and 3He targets [13]. Theoretical calculations in this kinematics have employed the parton picture and QCD interactions and produced a wide range of estimates [10, 14, 15, 16]. Further measurements at few-GeV energies are planned at Jeerson Lab [17]. Calculations

Email addresses: goity@jlab.org (J. L. Goity), weiss@jlab.org (C. Weiss), cintiawillemyns@gmail.com (C. Willemyns)

Preprint submitted to Elsevier

September 21, 2022

in the resonance region need to account for the contributions of individual hadronic channels to the inclusive cross section, including elastic scattering and resonance excitation, and require appropriate methods.

In this work we analyze the normal spin dependence of inclusive eN scattering in the resonance region using the 1=N_c expansion of QCD. The method organizes low-energy dynamics (hadron masses, couplings, form factors) based on the scaling properties in the limit of a large number of colors in QCD and has been successfully applied in many areas of hadronic physics [18, 19, 20, 21, 22, 23, 24]. Low-lying baryon states are organized in multiplets of the emerging contracted spin-flavor symmetry, with the baryon masses $O(N_c)$ and the splitting inside multiplets $O(N^{\ 1})$. The ground-state multiplet contains the N and , and transitions between them are governed by the symmetry and can be computed by expanding the transition operators in the group generators. In this way the parameters for the N– and – transitions are fixed in terms of measurable N-N transitions.

The 1=N_c expansion oers specific advantages for studying two-photon exchange and the normal spin dependence of inclusive scattering. The method treats N and states on the same basis and enables a consistent description of inelastic channels and inclusive scattering in resonance region. The group-theoretical techniques permit ecient calculation of the sums over channels in intermediate and final states. The parametric ordering of the kinematic variables gives rise to a physical picture that enables an intuitive understanding of the two-photon exchange process. Finally, the study of the N_c-scaling of the two-photon exchange observables can help to connect the resonance region with the DIS region and explain the transition between them.

In this letter we present the leading-order 1=N_c expansion and describe the calculational techniques and physical picture specific to this situation. A full analysis, including 1=N_c corrections and suppressed structures, will be presented elsewhere.

2. Method

2.1. Kinematics and final states

Inclusive electron scattering Eq. (1) is characterized by three independent kinematic variables, corresponding to the incident energy, the momentum transfer, and the energy transfer of the process. They can be chosen as the invariant variables

$$s \ \ (k_1 + p_1)^2 = (k_2 + p_2)^2; \qquad (5)\ t$$

$$(k_1 \ \ k_2)^2 = (p_2 \ \ p_1)^2 = q^2; \qquad (6)$$

$$m_X^2 = (q + p_1)^2 = p_2^2: \qquad (7)$$

In the following we use the CM frame, where the 3-momenta in the initial and final state are $p_1 = \ \ k_1 = P_1 n_1$; $p_2 = \ \ k_2 = P_2 n_2$, with $n_{1;2}$ unit vectors indicating the direction, and (m is the nucleon mass)

$$P_1 = \frac{\sqrt{s}}{2}\ \ \frac{m^2}{s}; \qquad P_2 = \frac{\sqrt{s}}{2}\ \ \frac{m_X^2}{s}; \qquad (8)$$

$$t = \ \ 2P_2P_1(1 \ \ n_2n_1): \qquad (9)$$

When analyzing the process Eq. (1) in the 1=N_c-expansion, we have to specify the scaling behavior of the kinematic variables in the parameter 1=N_c. Dierent choices are possible, leading to dierent types of expansions. Here we consider the domain where the CM momenta in the initial and final state are

$$P_1; P_2 \ = \ O(N_c^0); \qquad (10)$$

and final-state masses are such that

$$m_X \ \ m \ = \ O(N_c^{\ 1}); \qquad m; m_X \ = \ O(N_c): \qquad (11)$$

In this domain the only accessible final states are ground-state baryon multiplet containing the N and states,

$$X = N; : \qquad (12)$$

Other baryon multiplets, as well as N states, have masses m_X $m = O(N_c^0)$ and are not accessible as final states. Furthermore, Eqs. (10) and (11), together with Eq. (8), imply that

$$P_2 \ \ P_1 \ = \ \frac{m^2 \ \ m_X^2}{2\sqrt{s}} \ = \ O(N_c^{\ 1}) \ \ P_{1;2}: \qquad (13)$$

In leading order of 1=N_c we can therefore neglect the dierence between the initial and final CM momenta and write $P_1 = P_2 \ \ P$. For reference we note that, in this domain,

$$\sqrt{s} = O(N_c); \qquad \sqrt{s} \ \ m = O(N_c^0); \qquad t = O(N_c^0): \qquad (14)$$

The parametric ordering in 1=N_c gives rise to an interesting physical picture of the scattering process. The electron with energy $O(N_c^0)$ scatters from the heavy nucleon with mass $O(N_c)$, losing a small fraction $O(N_c^{\ 1})$ of its energy. The nucleon remains in ground state or gets excited to a by absorbing a small energy $O(N_c^{\ 1})$. The can be regarded as stable at this order (its width is negligible), and inelastic scattering consists simply in the transition from N to . The velocity of the initial/final baryons is small $O(N_c^{\ 1})$, and their kinetic energy is negligible compared to the electron energy. However, the momentum transfer is $O(N_c^0)$, so that the process probes the internal structure of the baryons. This picture will be further substantiated in the following calculations.

2.2. Currents and amplitudes

In the group-theoretical formulation of large-N_c QCD, the N and are described as states in the multiplet of ground-state baryons, characterized by the spin/isospin $S = I = 1{=}2$ and $3{=}2$, the spin projection S^3, and the isospin projection I^3, denoted collectively by B fS = I; S^3; I^3g. The electron scattering process takes the form of a transition between baryon states $hB_2j{:::}jB_1i$. We denote the electron-baryon scattering amplitude in the CM frame (with relativistic normalization) by

$$M(P; n_2; n_1j; B_2; B_1) \ \ M_{21}: \qquad (15)$$

is the electron helicity (i.e., the spin projection on n_1 and n_2), which is conserved in the scattering process. Note that the baryon spins are quantized along a fixed direction (the 3-direction in the CM frame); in this way the initial and final states have the same quantization axis, and the spin transitions can be computed using algebraic identities [23, 24].

The amplitude Eq. (15) can be computed as an expansion in the electromagnetic coupling,

$$M_{21} = M^{(e2)}_{21} + M^{(e4)}_{21} + \ldots \quad (16)$$

The e^2 term (one-photon exchange) is given by the product of the electron and baryon currents,

$$M^{(e2)}_{21} = -\frac{e^2}{t_{21}} (j)_{21} (J)_{21}; \quad (17)$$

$$(j)_{21} = \langle n_2; | j | n_1; \rangle; \quad (18)$$

$$(J)_{21} = \langle n_2; B_2 | J | n_1; B_1 \rangle; \quad (19)$$

where all particles have the common CM momentum P in leading order of $1/N_c$. The minus sign in Eq. (17) comes from the negative electric charge of the electron. The electron current Eq. (18) is the standard current of the spin-1/2 particle; its explicit form can be derived from the spinors in the CM frame. The baryon current Eq. (19) can be constructed using the large-N_c spin-flavor symmetry and expanded in the generators $\{1; I^a; S^i; G^{ia}\}$ [23, 24]. Their matrix elements are

$$\langle B_2 | \{1; I^a; S^i\} | B_1 \rangle = O(N_c^0); \qquad \langle B_2 | G^{ia} | B_1 \rangle = O(N_c): \quad (20)$$

The full $1/N_c$ expansion of the current is given in Ref. [25]. In the present calculation we focus on the leading-order contribution to the cross sections, which is produced by the isovector magnetic current proportional to G^{i3}. This current is given by

$$(J^0)_{21} = 0; \quad (21)$$

$$(J^i)_{21} = 2mp\, G^V_M(t_{21}) \, (-i)\epsilon^{ijk} (n_2 - n_1)^j \langle B_2 | G^{k3} | B_1 \rangle: \quad (22)$$

The factor 2m results from the relativistic normalization of the baryon states and drops out in final results. Note that Eq. (22) satisfy the transversality condition $q(J)_{21} = 0$ for all transitions between multiplet states, without corrections in $1/N_c$.

The function $G^V_M(t)$ in Eq. (22) (dimension mass^{-1}) is the large-N_c form factor, which describes the dynamical response of the large-N_c baryon to the momentum transfer $t_{12} = O(N_c^0)$. It can be determined by matching the $N \rightarrow N$ matrix element of the large-N_c current Eq. (22) with the empirical nucleon current at $N_c = 3$. At leading order in $1/N_c$ one obtains

$$2m\, G^V_M(t) \left.\frac{N_c}{6}\right|_{N_c=3} = \mathcal{G}^V_M(t); \quad (23)$$

where $\mathcal{G}^V_M(t)$ is the empirical isovector magnetic form factor, with $\mathcal{G}^V_M(0) = \frac{1}{2}(\mu_p - \mu_n)$ ($\mu_{p,n}$ are the magnetic moments of the proton and neutron). In this way the spin-flavor symmetry fixes the $N \rightarrow \Delta$ and $\Delta \rightarrow \Delta$ form factors in terms of the empirical $N \rightarrow N$ form factor, showing the predictive power of the $1/N_c$ expansion.

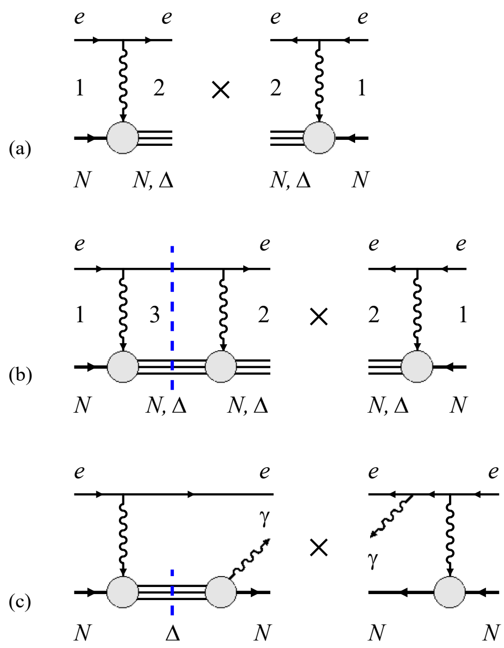

Figure 1: Inclusive eN scattering in the $1/N_c$ expansion in the domain Eqs. (10) and (11). (a) Spin-independent cross section from square of e^2 amplitudes. (b) Spin-dependent cross section from interference of e^4 and e^2 amplitudes. (c) Interference of real photon emission from electron and baryon.

The e^4 term in the electron-baryon scattering amplitude Eq. (16) results from two-photon exchange interactions. The absorptive part arises from on-shell rescattering and can be computed as the product of two e^2 amplitudes, integrated over the phase space of the intermediate state (see Fig. 1b),

$$M^{(e4)}_{21} = \frac{(-i)P}{8m} \int \frac{d\Omega_3}{4\pi} \sum_{B_3} M^{(e2)}_{23} M^{(e2)}_{31}: \quad (24)$$

We use the shorthand notation Eq. (15) for the amplitudes of the $1 \rightarrow 3$ and $3 \rightarrow 2$ transitions. The integral is over the momen-tum direction n_3 in the intermediate state 3, and the summation over the full set of baryon quantum numbers B_3, including N and and their spin/isospin projections. The form of Eq. (24) has been simplified according to the large-N_c limit.

The energies reached in the intermediate states in integral Eq. (24) extend up to $\sqrt{s} - m = O(N_c^0)$, which is parametrically larger than the mass of the final states considered in our domain, $m_X - m = O(N_c^{-1})$, Eq. (11). In principle therefore excited bayon states with mass dierence $m_B - m = O(N_c^0)$ (N states) can contribute to the two-photon exchange amplitude in our domain. However, the electromagnetic couplings of these states to the ground state multiplet are suppressed by $1/N_c$ relative to those between ground state baryons []. In leading order of the $1/N_c$ expansion it is thus justified to retain only ground state baryons N and as intermediate states.

The two-photon exchange amplitude Eq. (24) is free of collinear divergences, because the large-N_c baryon currents in the $1 \rightarrow 3$ and $3 \rightarrow 2$ amplitudes satisfy the transversality conditions without corrections in $1/N_c$ [10]

2.3. Cross section

Cross section for inclusive eN scattering Eq. (1) in the $1{=}N_c$ expansion in the domain Eq. (10) and (11) is obtained from the amplitude Eq. (15) as

$$\frac{d}{d_2} = \frac{1}{64^2 m^2} \frac{1}{2} \sum_{30\ 3} \sum_{S_1 S_1} (S_1^3; S_1^{30}) \sum_{B_2} M_{21}(; B_2; B_1)^{\dagger} M_{21}(; B_2; B_1): \quad (25)$$

We write the cross section as dierential in the solid angle of n_2, similar to elastic scattering. The inclusive scattering is expressed through the summation over the final baryon states $B_2 = N;$. The initial baryon is a nucleon, $B_1 = f\frac{1}{2}; S_1^3; I_1^3 g$ and $B_1^0 = f\frac{1}{2}; S_1^{30}; I_1^3 g$, with $I_1^3 = \frac{1}{2}$ for proton/neutron. The spin projections are averaged with the nucleon spin density matrix , which is normalized as tr $= 1$. It consists of an unpolarized and a polarized part, $= _U + _N$. The unpolarized part is

$$_U = \frac{1}{2}(S_1^3; S_1^{30}); \quad (26)$$

In the case of polarization along the unit vector e_N, Eq. (3), the polarized part is (^{i} are the Pauli matrices)

$$_N = \frac{1}{2} e_N (S_1; S_1^{30}); \quad (27)$$

such that the expectation value of the spin operator in the state is

$$\sum_{S_1^{30} S_1^3} {}_N hS_1^{30} jSjS_1^3 i = \frac{1}{2} e_N: \quad (28)$$

The spin-independent cross section in Eq. (2) is obtained from the product of e^2 amplitudes in Eq. (25) and given by (see Fig. 1a)

$$\frac{d_U}{d_2} = \frac{1}{64^2 m^2} \frac{1}{2} \sum \frac{1}{2} \sum_{S_1^3} \sum_{B_2} M_{21}^{(e2)} M_{21}^{(e2)}; \quad (29)$$

the expression will be evaluated further below. For the spin-dependent cross section, one can easily verify that it is zero at the same order in e^2, because the e^2 amplitude is real and the average with the density matrix $e_N = {}^y$ requires an imaginary part in one of the amplitudes (this is how the Christ-Lee theorem [11] is realized in our formulation). The spin-dependent cross section appears instead from the product of e^2 and e^4 amplitudes, i.e., the interference of one- and two-photon exchange (see Fig. 1b)

$$\frac{d_N}{d_2} = \frac{1}{64^2 m^2} \frac{1}{2} \sum_{30\ 3} \sum_{S_1 S_1} {}_N d \sum_{B_2} \left[M_{21}^{(e2)} M_{21}^{(e4)} + M_{21}^{(e4)} M_{21}^{(e2)} \right]: \quad (30)$$

With the e^4 amplitude given by Eq. (24), the spin-dependent cross section is completely expressed in terms of the e^2 amplitude Eq. (17), and thus in terms of the large-N_c baryon current matrix elements.

3. Results

3.1. Spin-dependent cross section and asymmetry

We now extract the leading $1{=}N_c$ term of the spin-dependent cross section. It results from the isovector magnetic current Eq. (22) proportional to spin-flavor generator G^{i3}. The e^2 amplitude Eq. (17) produced by this current is

$$M_{21}^{(e2)} = \frac{e^2 G_{M21}^V}{2P^2(1 \quad n_2 n_1)} a_{21}^i hB_2 jG^{i3} jB_1 i; \quad (31)$$

$$a_{21} \quad a_{21}(n_2; n_1;) \ (\ i)(n_2 \quad n_1) \ j_{21}; \quad (32)$$

where j_{21} is the spatial part of the electron current Eq. (18). The product of e^2 and e^4 amplitudes in Eq. (30) then becomes

$$M_{21}^{(e2)} M_{21}^{(e4)} = \frac{(\ i)P_V}{8m} \int \frac{d}{4} G_{M21} G_{M23}^V G_{M31}^k \ j a_{21}^i a_{23} a_{31} \sum_{B_2} \sum_{B_3} h B_1^0 \ jG^{k3} jB_2 i hB_2 jG^{j3} jB_3 i hB_3 jG^{i3} jB_1 i: \quad (33)$$

It represents a sequence of isovector magnetic transitions, with a tensor structure governed by the electron current and the transition geometry. We evaluate it using algebraic methods based on t-channel angular momentum considerations []. For the intermediate states in the e^4 amplitude, we sum over $B_3 = N;$ using the completeness relation in ground state representation

$$\sum_{B_3} jB_3 i hB_3 j = 1; \quad (34)$$

and the product on the last line of Eq. (33) becomes

$$\sum_{B_2} h B_1^0 jG^{k3} jB_2 i hB_2 jG^{j3} G^{i3} jB_1 i: \quad (35)$$

For the final states, we distinguish two cases:

(i) Nucleon final state, $B_2 = N$. In this case the matrix element of $G^{i3} G^{j3}$ in Eq. (35) is a $\frac{1}{2}$! $\frac{1}{2}$ spin transition, and the tensor formed by the operator product can only have t-channel angular momentum $J = 0$ or 1. The $J = 1$ part, antisymmet-ric in ij, is suppressed in $1{=}N_c$ because the commutator of the operators is $[G^{i3}; G^{j3}] = O(N_c^0)$. The tensor can therefore be projected on $J = 0$ (we show only leading term in $1{=}N_c$)

$$G^{j3} G^{i3} \ ! \ \frac{1}{3} {}^{ji} G^{l3} G^{l3} = \frac{1}{3} {}^{ji} \frac{N_c^2}{16}; \quad (36)$$

and Eq. (35) becomes

$$\frac{1}{3} {}^{ji} \frac{N_c^2}{16} hB_1^0 jG^{k3} jB_1 i: \quad (37)$$

(ii) Sum of nucleon and Delta final states, $B_2 = N +$. In this case the summation over B_2 can be performed with the completeness relation [see Eq. (34)], and Eq. (35) becomes

$$hB_1^0 jG^{k3} G^{j3} G^{i3} jB_1 i \quad T^{kji}: \quad (38)$$

Because the commutator of the G operators is suppressed in $1{=}N_c$, see above, the tensor T^{kji} can be regarded as completely symmetric in leading order. As such it can be projected on overall J = 1 using

$$T^{kji} \; ! \; \frac{1}{5}({}^{kj}T^{i} + {}^{ki}T^{j} + {}^{ji}T^{k}); \quad (39)\ T^{k}$$

$$T^{kll} = \frac{N_c^2}{16} hB_1^0 jG^{k3} jB_1 i: \quad (40)$$

The two cases thus lead to similar contractions of the tensor Eq. (35). The remaining matrix element of G^{k3} in Eqs. (37) and (40) is proportional to the initial nucleon spin and and isospin and evaluates to (in leading order of $1{=}N_c$)

$$hB_1^0 jG^{k3} jB_1 i = \frac{N_c}{6} hS_1^{30} jS^{k} jS_1^{3} i\,(2I_1^3); \quad (41)$$

which can be averaged with the spin density matrix in Eq. (33). Altogether, we obtain the spin-dependent cross section in leading order of $1{=}N_c$

$$\frac{d_N}{d} = \frac{(2I_1^3)\ {}^3 N^3\ P\ G^V_{M21}}{96(1}$$

$$^2\ n_2 n_1)^{3=2} (1 + n_2 n_1)^{1=2}\ Z\ \ d \; : \quad (42)$$

$$^3\ \frac{G_{M23} G_{M31}}{4\ (1 \quad n_2 n_3)(1 \quad n_3 n_1)}$$

$$= [::] \frac{1}{2} \sum e_N (a^k_{21} a^k_{23} a^l_{31}{}^l + \text{C.C.}) \quad [\text{final } N]; \quad (43)$$

$$= [::] \frac{1}{2} \sum e^{k}_{N} (a^k_{21} a_{23} a^l_{31} + a^l_{21} a_{23} a^k_{31}{}^l$$

$$+ a^l_{21} a^l_{23} a^k_{31} + \text{C.C.}) \quad [\text{final } N +]: \quad (44)$$

Here $e^2{=}4$ is the fine structure constant. The angular func-tions can be evaluated using the specific form Eq. (32) of the axial vectors a^i_{21}; a^i_{23} and a^i_{31}; explicit formulas will be pre-sented elsewhere. The spin-dependent cross section Eq. (42) is proportional to initial nucleon isospin $(2I_1^3) = 1$ and has dierent sign for ep and en scattering

$$d_N = d_N[ep] = \quad d_N[en]: \quad (45)$$

We can also compute spin asymmetry

$$A_N \quad \frac{d_N}{d} \,{}' \, \frac{d_U}{d} \quad {}^2 \; ; \quad (46)$$

by dividing by the unpolarized cross section computed in the same approximation. In leading order of $1{=}N_c$, the unpolarized cross section Eq. (29) arises from the isovector magnetic current in the e^2 amplitude. In the case of summation over N and final states, B_2 = N; , the result is

$$\frac{d_U}{d} = \frac{{}^2 N_c^2 (G^V_{M2})^2}{192\, P^2 (1 \quad n_2 n_1)^2} \frac{1}{2} \sum a^i_{21} a^i_{21} \quad (47)$$

$$= \frac{{}^2 N_c^2 (3 \quad n_2 n_1)(G^V_{M21})^2}{48\,(1 \quad n_2 n_1)}: \quad (48)$$

The spin-independent cross section Eq. (48) is independent of the initial nucleon isospin; the asymmetry Eq. (46) therefore

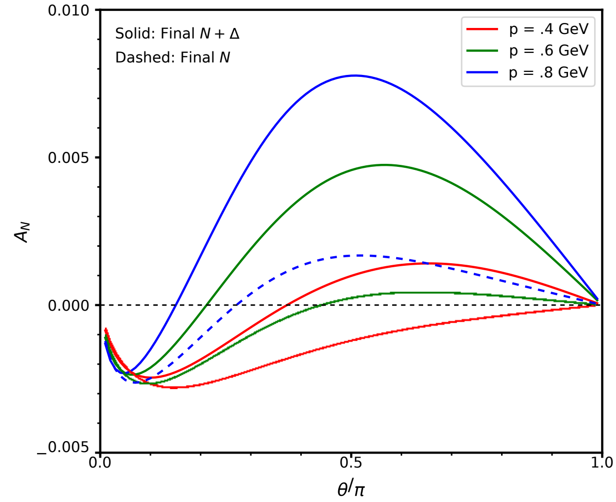

Figure 2: Transverse normal single-spin asymmetry in inclusive eN scattering, Eq. (46), in leading order of the $1{=}N_c$ expansion, for several CM energies P, as a function of . Dashed lines: A_N with N final state in $_N$ in the numerator. Solid lines: A_N with N + final states in $_N$. In both cases, $_U$ in the denominator is the sum N + .

has the same isospin dependence as the spin-dependent cross section in the numerator,

$$A_N = A_N[ep] = \quad A_N[en]: \quad (49)$$

Some comments on these result from the perspective of the $1{=}N_c$ expansion. First, the spin-dependent cross section is parametrically large in N_c, as it appears from the maximal product of isovector magnetic currents with matrix elements $O(N_c)$. Second, our calculation provides an example of the "I = J rule" of large-N_c QCD, according to which leading structures appear with t-channel quantum numbers I = J. The spin-dependent cross section (as a matrix element between the nucleon states 1) is a structure with overall J = 1, and its leading large-N_c result has I = 1. It arises as the product of an e^2 amplitude with I = J = 1 (for both final N and) with an e^4 amplitude that is either projected on total I = J = 0 (for final N) or on I = J = 2 (for final), as can be observed in the algebraic calculation above.

3.2. Numerical results

We now evaluate the asymmetry numerically and study its kinematic dependence using the leading-order $1{=}N_c$ expansion results, Eqs. (42)–(44) and Eq. (48). The large-N_c form factors $G^V_M(t)$ appearing in the expressions are fixed by the matching condition Eq. (23), and we use the standard dipole $1{=}(1 \quad t{=}0{:}71\,\text{GeV}^2)^2$ to model the empirical t-dependence.

Figure 2 shows A_N for several values of P . 1 GeV as a function of = angle($n_2 n_1$). Results are shown for the cases of N and N + final states in $_N$ in the numerator; $_U$ in the denominator is always for N + final states; in this way one can add/subtract the results for A_N in the graph and see the contributions of the various channels to $_N$. (The intermediate states in the two-photon exchange amplitude in $_N$ are always N + .)

One observes: (i) A_N vanishes at = 0 and , which is nat-ural, as at these angles the normal vector n_2 n_1 vanishes. (ii) The contribution of final states (the dierence of the results for N + and N final states) is small at small but becomes sig-nificant at =2, causing the A_N for final N + to be several times larger than that for final N. (iii) A_N reaches values of the order 10^{2} at =2 and P 1 GeV and has definite sign.

Some comments on the region of applicability of the large-N_c expressions. First, the present 1=N_c expansion refers to the parametric domain Eq. (11) and assumes that the channel is open; the expressions should therefore be applied at CM energies above the empirical threshold, $\sqrt{s}$ m P > (m m)[empirical] = 0:3 GeV. Second, the leading-order results for $_N$ and A_N arise entirely from magnetic transitions, which are proportional to the momentum transfer at the vertices. They are not expected to be accurate at small =2 and P 1 GeV, where the momentum transfer is kinematically suppressed, and corrections from electric currents are large (those can be computed as part of the 1=N_c corrections). Altogether, we expect the leading 1=N_c expansion to be a fair approximation at large angles =2 and momenta P 0.5–1 GeV. The accuracy in this domain can be expected to be of the typical accuracy of the 1=N_c expansion in hadronic observables [].

4. Extensions

We have computed the target normal single-spin asymmetry in inclusive eN scattering in leading order of the 1=N_c expansion, in the parametric domain where the energy transfer is $O(N_c^{1})$ and allows for excitation of N and final states, and the momentum transfer is $O(N_c^0)$ and probes the internal structure of the baryons. The results of the present study can be extended and applied in several ways.

The method developed here, particularly algebraic approach in Sec. 3, can be used to compute 1=N_c corrections to leading-order result in the same parametric domain. These corrections will quantify the numerical accuracy of the leading-order result for the isovector $_N$, and provide estimates of the isoscalar $_N$, which appears only at subleading order.

The cross section for inclusive eN scattering includes also real photon emission into the final state (Fig. 1c). The process can be analyzed in 1=N_c expansion in the same manner as two-photon exchange (Fig. 1b). Preliminary analysis suggests that the emission cross section is suppressed in 1=N_c, because the emitted photon is soft, p = $O(N_c^{1})$, and the emission through the leading magnetic vertex is suppressed. A full analysis of the real emission process will be presented elsewhere.

The 1=N_c expansion can also be performed in dierent parametric domains than Eqs. (10) and (11). For example, the choice P = $O(N_c^{1})$ leads to a "low-energy expansion" in which the electric currents enter in the same order as the magnetic ones, giving rise to dierent physical picture.

The results of the present study can be used to study the transition between the resonance and DIS regions and the realization of quark-hadron duality in the target normal single-spin asymmetry. Theoretical estimates of A_N dier by up to 1-2 orders of magnitude between the resonance and DIS regions, because of large eects of anomalous magnetic moment that are present in the resonance region but disappear in the DIS region. The N_c scaling behavior and the "mean field picture" emerging in the large-N_c limit may help to explain the transition. (For applications of the 1=N_c expansion to DIS and partonic structure, see Refs. [26, 27].)

The methods developed here could also be applied to the beam spin asymmetry in electron-nucleon scattering, an eect proportional to the electron mass, which is being studied in its own right and as a background to parity-violating electron scattering [28, 29, 30]; and to other observables in electron-nucleon scattering.

This material is based upon work supported by the U.S. Department of Energy, Oce of Science, Oce of Nuclear Physics under contract DE-AC05-06OR23177.

References

References

[1] C. E. Carlson, M. Vanderhaeghen, Two-Photon Physics in Hadronic Processes, Ann. Rev. Nucl. Part. Sci. 57 (2007) 171–204. arXiv:hep-ph/0701272, doi:10.1146/annurev.nucl.57.090506.123116.

[2] M. K. Jones, et al., $G_{Ep}=G_{Mp}$ ratio by polarization transfer in ep ! ep, Phys. Rev. Lett. 84 (2000) 1398–1402. arXiv:nucl-ex/9910005, doi:10.1103/PhysRevLett.84.1398.

[3] P. A. M. Guichon, M. Vanderhaeghen, How to reconcile the Rosenbluth and the polarization transfer method in the measurement of the proton form-factors, Phys. Rev. Lett. 91 (2003) 142303. arXiv:hep-ph/0306007, doi:10.1103/PhysRevLett.91.142303.

[4] P. G. Blunden, W. Melnitchouk, J. A. Tjon, Two photon exchange and elastic electron proton scattering, Phys. Rev. Lett. 91 (2003) 142304. arXiv:nucl-th/0306076, doi:10.1103/PhysRevLett.91.142304.

[5] B. S. Henderson, et al., Hard Two-Photon Contribution to Elastic Lepton-Proton Scattering: Determined by the OLYMPUS Experiment, Phys. Rev. Lett. 118 (9) (2017) 092501. arXiv:1611.04685, doi:10.1103/PhysRevLett.118.092501.

[6] J. C. Bernauer, et al., Measurement of the Charge-Averaged Elastic Lepton-Proton Scattering Cross Section by the OLYMPUS Experiment, Phys. Rev. Lett. 126 (16) (2021) 162501. arXiv:2008.05349, doi:10.1103/PhysRevLett.126.162501.

[7] A. Accardi, et al., An experimental program with high duty-cycle polarized and unpolarized positron beams at Jeerson Lab, Eur. Phys. J. A 57 (8) (2021) 261. arXiv:2007.15081, doi:10.1140/epja/s10050-021-00564-y.

[8] E. Cline, et al., Characterization of Muon and Electron Beams in the Paul Scherrer Institute PiM1 Channel for the MUSE Experiment (9 2021). arXiv:2109.09508.

[9] A. V. Afanasev, C. E. Carlson, Two-photon-exchange correction to parity-violating elastic electron-proton scattering, Phys. Rev. Lett. 94 (2005) 212301. arXiv:hep-ph/0502128, doi:10.1103/PhysRevLett.94.212301.

[10] A. Afanasev, M. Strikman, C. Weiss, Transverse target spin asymmetry in inclusive DIS with two-photon exchange, Phys. Rev. D 77 (2008) 014028. arXiv:0709.0901, doi:10.1103/PhysRevD.77.014028.

[11] N. Christ, T. D. Lee, Possible Tests of C_{st} and T_{st} Invariances in l + N ! l + and A ! B + e + e , Phys. Rev. 143 (1966) 1310–1321. doi:10.1103/PhysRev.143.1310.

[12] A. Airapetian, et al., Search for a Two-Photon Exchange Contribution to Inclusive Deep-Inelastic Scattering, Phys. Lett. B 682 (2010) 351–354. arXiv:0907.5369, doi:10.1016/j.physletb.2009.11.041.

[13] J. Katich, et al., Measurement of the Target-Normal Single-Spin Asymmetry in Deep-Inelastic Scattering from the Reaction $^3He^{\uparrow}(e, e')X$, Phys. Rev. Lett. 113 (2) (2014) 022502. arXiv:1311.0197, doi:10.1103/PhysRevLett.113.022502.

[14] A. Metz, M. Schlegel, K. Goeke, Transverse single spin asymmetries in inclusive deep-inelastic scattering, Phys. Lett. B 643 (2006) 319–324. arXiv:hep-ph/0610112, doi:10.1016/j.physletb.2006.11.009.

[15] A. Metz, D. Pitonyak, A. Schafer, M. Schlegel, W. Vogelsang, J. Zhou, Single-spin asymmetries in inclusive deep inelastic scattering and multiparton correlations in the nucleon, Phys. Rev. D 86 (2012) 094039. arXiv:1209.3138, doi:10.1103/PhysRevD.86.094039.

[16] M. Schlegel, Partonic description of the transverse target single-spin asymmetry in inclusive deep-inelastic scattering, Phys. Rev. D 87 (3) (2013) 034006. arXiv:1211.3579, doi:10.1103/PhysRevD.87.034006.

[17] G. N. Grauvogel, T. Kutz, A. Schmidt, Target-normal single spin asymmetries measured with positrons, Eur. Phys. J. A 57 (6) (2021) 213. arXiv:2103.05205, doi:10.1140/epja/s10050-021-00531-7.

[18] G. 't Hooft, A Planar Diagram Theory for Strong Interactions, Nucl. Phys. B 72 (1974) 461. doi:10.1016/0550-3213(74)90154-0.

[19] E. Witten, Baryons in the 1=N Expansion, Nucl. Phys. B 160 (1979) 57–115. doi:10.1016/0550-3213(79)90232-3.

[20] J.-L. Gervais, B. Sakita, Large-N QCD Baryon Dynamics: Exact Results from Its Relation to the Static Strong Coupling Theory, Phys. Rev. Lett. 52 (1984) 87. doi:10.1103/PhysRevLett.52.87.

[21] J.-L. Gervais, B. Sakita, Large-N Baryonic Soliton and Quarks, Phys. Rev. D 30 (1984) 1795. doi:10.1103/PhysRevD.30.1795.

[22] R. F. Dashen, A. V. Manohar, Baryon-pion couplings from large-N_c QCD, Phys. Lett. B 315 (1993) 425–430. arXiv:hep-ph/9307241, doi:10.1016/0370-2693(93)91635-Z.

[23] R. F. Dashen, E. E. Jenkins, A. V. Manohar, 1=N_c expansion for baryons, Phys. Rev. D 49 (1994) 4713, [Erratum: Phys.Rev.D 51, 2489 (1995)]. arXiv:hep-ph/9310379, doi:10.1103/PhysRevD.51.2489.

[24] R. F. Dashen, E. E. Jenkins, A. V. Manohar, Spin flavor structure of large N_c baryons, Phys. Rev. D 51 (1995) 3697–3727. arXiv:hep-ph/9411234, doi:10.1103/PhysRevD.51.3697.

[25] I. P. Fernando, J. L. Goity, SU(3) vector currents in baryon chiral perturbation theory combined with the 1=N_c expansion, Phys. Rev. D 101 (5) (2020) 054026. arXiv:1911.00987, doi:10.1103/PhysRevD.101.054026.

[26] D. Diakonov, V. Petrov, P. Pobylitsa, M. V. Polyakov, C. Weiss, Nucleon parton distributions at low normalization point in the large-N_c limit, Nucl. Phys. B 480 (1996) 341–380. arXiv:hep-ph/9606314, doi:10.1016/S0550-3213(96)00486-5.

[27] P. Schweitzer, D. Urbano, M. V. Polyakov, C. Weiss, P. V. Pobylitsa, K. Goeke, Transversity distributions in the nucleon in the large-N_c limit, Phys. Rev. D 64 (2001) 034013. arXiv:hep-ph/0101300, doi:10.1103/PhysRevD.64.034013.

[28] A. V. Afanasev, N. P. Merenkov, Collinear photon exchange in the beam normal polarization asymmetry of elastic electron-proton scattering, Phys. Lett. B 599 (2004) 48. arXiv:hep-ph/0407167, doi:10.1016/j.physletb.2004.08.023.

[29] C. E. Carlson, B. Pasquini, V. Pauk, M. Vanderhaeghen, Beam normal spin asymmetry for the ep ! e(1232) process, Phys. Rev. D 96 (11) (2017) 113010. arXiv:1708.05316, doi:10.1103/PhysRevD.96.113010.

[30] O. Koshchii, A. Afanasev, Lepton mass eects for beam-normal single-spin asymmetry in elastic muon-proton scattering, Phys. Rev. D 100 (9) (2019) 096020. arXiv:1905.10217, doi:10.1103/PhysRevD.100.096020.